Journal of Medicinal Chemistry

ARTICLE

pubs.acs.org/jmc

Cytotoxic 1,2-Dialkynylimidazole-Based Aza-Enediynes: Aza-Bergman Rearrangement Rates Do Not Predict Cytotoxicity

Christophe Laroche, Jing Li, and Sean M. Kerwin*

Division of Medicinal Chemistry, College of Pharmacy, The University of Texas at Austin, Texas 78712, United States

Supporting Information

ABSTRACT:

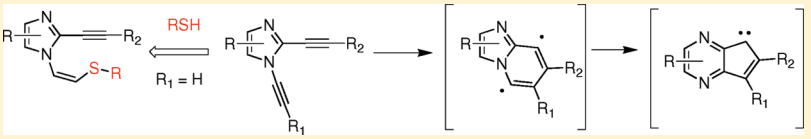

A new class of potential antitumor agents inspired by the enediyne antitumor antibiotics has been synthesized: the 1,2-dialkynylimidazoles. The aza-Bergman rearrangement of these 1,2-dialkynylimidazoles has been investigated theoretically at the B3LYP/6-31G(d,p) level and experimentally by measuring the kinetics of rearrangement in 1,4-cyclohexadiene. There is a good correlation between the theoretical and experimental results; subtle substituent effects on the initial aza-Bergman cyclization barrier predicted by theory are confirmed by experiment. Yet, despite the ability of these 1,2-dialkynylimidazoles to undergo Bergman rearrangement to diradical/carbene intermediates under relatively mild conditions, there is no correlation between the rate of Bergman cyclization and cytotoxicity to A459 cells. In addition, cytotoxic 1,2-dialkynylimidazoles do not cause nicking of supercoiled plasmid DNA or cleavage of bovine serum albumin. An alternative mechanism for cytotoxicity involving the unexpected selective thiol addition to the *N*-ethynyl group of certain 1,2-dialkynylimidazoles is proposed.

INTRODUCTION

The extreme cancer cell cytotoxicity of natural enediyne compounds such as calcheamicin γ_1,[1] esperamicin A_1,[2] or dynemicin A[3] involves DNA cleavage via diradical intermediates arising from the cyclization of the enediyne core.[4] In order to address the selectivity issues associated with these natural products, a wide variety of enediyne analogues have been prepared and examined for DNA cleavage and cancer cell cytotoxicity activities.[5−8] In this respect, computational chemistry has substantially aided in the design of enediynes that undergo diradical-generating Bergman cyclization under physiological conditions.[9−13]

Recently, several enediynes have been described that do not undergo Bergman cyclization under physiological conditions, but which still display interesting cancer cell cytotoxicity.[14] These enediynes induce G2/M cell cycle arrest by targeting microtubule formation,[14a] although other targets such as topoisomerase I and MAPK pathways have also been proposed.[14b,c]

Following the initial report of the aza-Bergman cyclization of *C*,*N*-dialkynylimines,[15a] these and related aza-enediynes have been explored as potential DNA-cleaving anticancer agents with improved selectivity compared to that of the enediynes.[15−17] Numerous computational studies have been carried out with the aim of designing aza-enediynes that might undergo a pH-dependent switch in reactivity mediated by changes in the kinetic stability and reactivity of the diradical upon nitrogen atom protonation.[18−20] Although DNA cleavage agents based upon the aza-Myers-Saito cyclization[20] have been reported,[22] no reports of DNA cleavage from the aza-Bergman cyclization pathway have been published.

1,2-Dialkynylimidazoles (**1**) have been investigated as a class of aza-enediynes (Figure 1).[23] Mild thermolysis of 1,2-dialkynylimidazoles under neutral conditions affords products (e.g., cyclopropanes **3**, Figure 1) derived from the trapping of cyclopentapyrazine carbene intermediates **C**.[23a] It has been proposed, on the basis of DFT calculations, that these arise from the cyclization of cyclic cumulene **B** formed by the collapse of the aza-Bergman cyclization-derived diradical intermediate **A** (Figure 1).[23b] In contrast, themolysis of dialkynylimidazoles **1** in the presence of HCl, affords chloroimidazapyridine products **2** (Figure 1),[23c] formally derived from trapping a putative 5,8-didehydroimidazo-[1,2-a]pyridinium diradical **D** through nucleophilic attack.[24]

Recently, we reported the unique and potent cancer cell cytotoxicity of the 1,2-dialkynylimidazole **1a** (R = *p*-methoxyphenyl).[25] In order to better understand the structural basis and role of the thermal generation of diradical and/or carbene intermediates in the cytotoxicity demonstrated by **1a**, we have prepared a series of dialkynylimidazoles and related imidazoles and determined their cytotoxicity against A549 human nonsmall cell lung cancer cells. The aza-Bergman cyclization kinetics of selected dialkynylimidazoles were also studied experimentally and by DFT calculations. Interestingly, although some of these dialkynylimidazoles are very cytotoxic to A549 cells, the degree of cytotoxicity is unrelated to the kinetics of aza-Bergman cyclization. Furthermore, we find evidence that the 1-ethynylimidazole moiety contributes to the cytotoxicity of

Received: March 11, 2011
Published: June 13, 2011

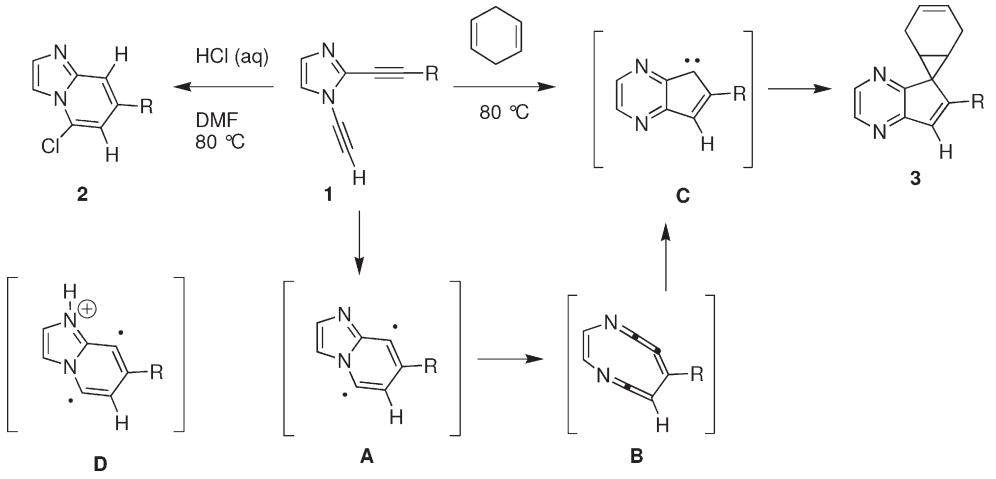

Figure 1. Thermolysis products derived from 1,2-dialkynylimidazoles.

these compounds, possibly as a result of the unexpected reactivity of this functionality with thiols.

RESULTS

Chemistry. The 1,2-dialkynylimidazoles **1a**−**p** were prepared from the corresponding, previously reported[27] 1-alkynyl-2-iodoimidazoles **4a**−**g**, which were coupled to a variety of terminal alkynes under standard Sonogashira coupling conditions, followed, if necessary, by silyl deprotection with TBAF in THF (Table 1).

Related alkynylimidazoles **5a**[26] and **5b**[27] (Scheme 1) were prepared as previously described. Deprotection of the silylalkynylimidazole **6a**[26] afforded the ethynylimidazole **6b**. The 1-methylimidazole **7** was prepared from 1-*tert*-butoxycarbonyl-2-iodoimidazole[28] by Sonogashira coupling, deprotection, and methylation (Scheme 1). Treating the dialkynylimidazole **1a** with thiophenol in THF at room temperature for 5 days afforded the addition product **8** as a single diastereomer that was assigned the (*Z*)-configuration on the basis of ^{1}H NMR coupling constants (8.4 Hz) for the alkenyl protons.

Computational Studies. The thermal rearrangements of 1,2-dialkynylimidazoles afford products formally derived from the trapping of the 5,8-didehydroimidazo[1,2-*a*]pyridine diradical or the 5,5-didehydro-5*H*-cyclopenta[*b*]pyrazine carbene intermediates, depending upon reaction conditions.[23] In both cases, the observed products are proposed to arise from an initial Bergman-type cyclization.[23] In order to investigate the potential of 1,2-dialkynylimidazoles to serve as diradical- or carbene-generating cytotoxic agents, computational studies of this Bergman-type cyclization and subsequent rearrangement were carried out for a number of representative substituted 1,2-dialkynylimidazoles.

Computational studies of the Bergman cyclization are challenging due to the multiconfigurational nature of the diradical species. Accurate descriptions of these species require addressing both dynamic and static electron correlation effects, and multireference or single-determinant methods incorporating a large degree of dynamic electron correlation are required.[29−31] However, these methods are too taxing for any but the most simple systems. Fortunately, unrestricted broken spin density functional theory can provide accurate energies for the Bergman rearrangement of enediynes.[12,32] Recently, Sherer and Shields compared the results of sum-corrected BS-UB3LYP/6-31G(dp) calculations with experimental activation energies for a wide range of enediynes and found that with few exceptions, the calculated reaction barriers were in quantitative agreement with the experiment.[33] In a preliminary report, we described the results of DFT calculations for the rearrangement **1** → **TS1** → **A** → **TS2** → **B** → **TS3** → **C** (Figure 2) for the 1,2-dialkynylimidazole **1a** employing this same approach.[25] The initial Bergman-type cyclization of **1a** to the 5,8-didehydroimidaza[1,2-*a*]pyridine diradical **A** was identified as the rate-determining step for the rearrangement on the basis of calculations. Significantly, the calculated energy of activation for the rearrangement of **1a** (29.7 kcal/mol) is in excellent agreement with the experimental value (30.0 kcal/mol).[25] Here, we employ this DFT approach to evaluate the effect of substituents on the energetics of the Bergman-type cyclization of 1,2-dialkynylimidazoles. These calculations are compared to experimentally determined rates to further validate this method and to determine if the rate of thermal rearrangement for a series of 1,2-dialkynylimidazoles is correlated with their cytotoxicity.

Molecular geometries for all species were optimized at the density functional theory (DFT) level of theory using the gradient-corrected exchange functional of Becke[34] and the hybrid HF gradient-corrected correlation functional of Lee, Yang, and Parr[35] (B3LYP) and the 6-31G(d,p) basis set. Calculation triplet states of biradicals and carbenes employed an unrestricted formalism. For singlet state biradicals **A** and the transitions states leading to (**TS1**) and from (**TS2**), these species calculations employed the broken-spin unrestricted formalism.[33,36] For diradicals **A** and **TS2**, this leads to substantial triplet contamination, with $\langle S^2 \rangle$ values of 0.88−0.89 for **A** and 0.47−0.48 for **TS2**. The energies for **A** and **TS2** were thus corrected for contamination by the higher energy triplet states using a sum-correction method employing the single-point triplet state energies calculated at the broken-spin singlet geometries for these species.[33,36] All calculations were carried out using Gaussian 03.[37]

Optimized structures for the starting 1,2-dialkynylimidazoles **1** bearing phenyl substituents (**1a**,**c**,**e**,**i**,**k**) were those having the phenyl substituent coplanar with the imidazole ring, as observed in the X-ray structure of **1a**;[25] however, no symmetry constraints were employed for these or any other species during optimization (C_1 symmetry). All geometries were verified as local minima or the appropriate saddle points by computation of analytic

Table 1. Synthesis of Dialkynylimidazoles 1a−p

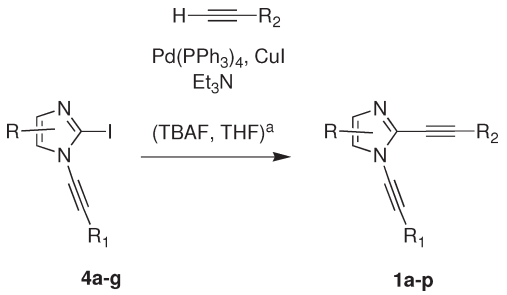

Starting Iodoimidazole	R =	R_1 =	R_2 =	Product (Yield)
4a[b]	H	H	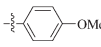	1a (75 %)[b]
4b[c]	H	H		1b (75 %)
4b[c]	H	H		1c (69 %)[c]
4b[c]	H	H	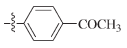	1d (73 %)
4b[c]	H	H	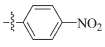	1e (71 %)
4b[c]	H	H	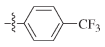	1f (69%)[h]
4b[c]	H	H	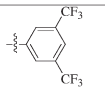	1g (68 %)
4b[c]	H	H		1h (70%)[c]
4c[d]	H	Ph	H	1i (63 %)[d]
4d[e]	H	CH_2OH	CH_2OH	1j (71 %)
4e[f]	Ph	H	H	1k (79 %)[d]
4e[f]	Ph	H	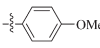	1l (78 %)[d]
4f[g]		H	H	1m (82 %)
4f[g]	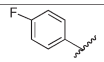	H	CH_2CH_2OH	1n (35 %)
4g[f]		H	H	1o (75 %)
4g[f]		H	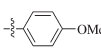	1p (92 %)

[a] An optional deprotection of silyl groups was carried out, except in the case of reactions of **4c**. [b] In **4a**, R = TIPS; see ref 25. [c] In **4b**, R = TMS; see ref 23c. [d] See ref 23d. [e] In **4c**, R = $CH_2OTBDMS$; see ref 23d. [f] In **4e**,**g**, R = TIPS; see ref 23d. [g] See ref 23c. [h] See ref 23b.

vibrational frequencies. The energies reported are electronic energies corrected by zero-point vibrational energies (E + ZPE) or thermal contributions to enthalpy at 298 K (H_{298}) computed from these unscaled frequencies.

Scheme 1. Synthesis of Related Alkynylimidazoles

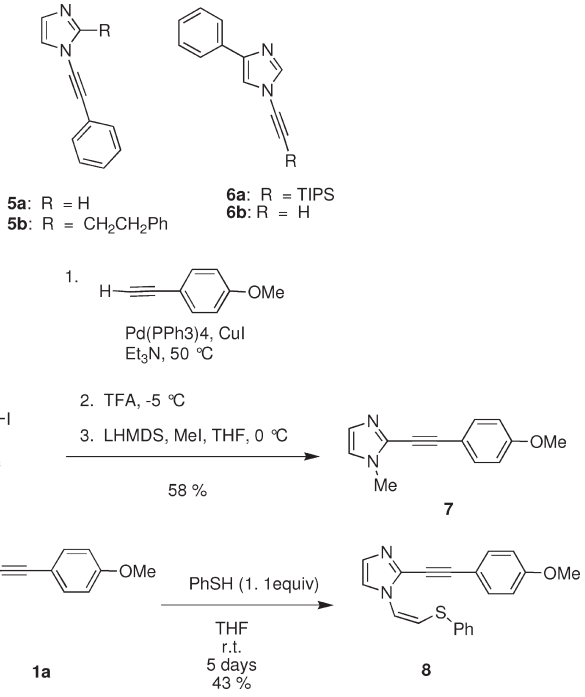

Calculations of the species involved in the initial Bergman cyclization (**1** → **TS1** → **A**, Figure 2) were carried out for the phenyl substituted 1,2-dialkynylimidazoles **1a**−**c**,**e**,**i**,**k** (Table 2). The species involved in the subsequent collapse of the diradicals and cyclization to the carbenes (**A** → **TS2** → **B** → **TS3** → **C**) were also examined (Table 2). In all of these cases, the initial Bergman cyclization (**TS1**) was identified as the rate-limiting step in the cascade.

There is a modest effect of the position of the phenyl substituent on the Bergman cyclization transition state (**TS1**) relative energy. The 4-substituted 1,2-dialkynylimidazole **1k** has a relatively low Bergman cyclization barrier of 25.9 kcal/mol (Table 2) that is identical with that calculated for the parent 1,2-diethynimidazole (see Supporting Information). Moving the phenyl substituent to either of the alkyne termini leads to an increase in the Bergman cyclization barrier, and this effect is more pronounced for the substitution on the 2-alkyne group (**1c**, 30.0 kcal/mol) compared to the substitution on the *N*-alkyne moiety (**1i**, 29.0 kcal/mol). Further substitution of the phenyl group of **1c** has an even more modest an effect on the Bergman cyclization barrier. While electron-donating substituents have little effect on the Bergman cyclization barrier (**1a** and **1b**, 29.9 kcal/mol), there is a slight increase in the barrier for the *p*-nitrophenyl substituted analogue **1e** (30.7 kcal/mol).

In order to address solvent effects on the Bergman cyclization rates of these substituted 1,2-dialkynylimidazoles, the calculated dipole moments of the reactants **1** and Bergman cyclization transition states (**TS1**) were examined (Table 3). In all but the case of the *p*-nitrophenyl-substituted analogue **1e**, the dipole moment of **TS1** is larger than that of **1**. This leads to the prediction that the Bergman cyclization barriers for these substituted 1,2-dialkynylimidazoles will be somewhat lower in polar solvents such as water when compared to those in nonpolar solvents due to increased solvation of the

dx.doi.org/10.1021/jm200289j |*J. Med. Chem.* 2011, 54, 5059–5069

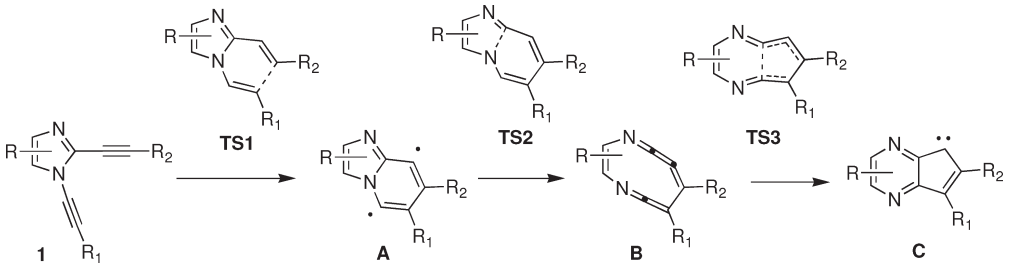

Figure 2. Aza-Bergman rearrangement of 1,2-dialkynylimidazoles.

Table 2. (U)B3LYP/6-31G(d,p) Absolute (h) and Relative (kcal/mol) Energies of Stationary Points along the Bergman Cyclization/Rearrangement Pathway for Substituted 1,2-Dialkynylimidazoles

	energy	TS1[a]	A[a]	S-T[b]	TS2[c]	B[a]	TS3[d]	C[a]
1a	−723.8899378	29.9	12.2	9.3	1.3 (20.7)	−7.2	14.7	3.3
1b	−766.5503445	29.9	12.0	9.2	1.3 (20.6)	−7.3	14.8	3.4
1c	−609.3964804	30.0	12.0	9.3	1.2 (20.5)	−7.3	14.8	3.4
1e	−813.8931719	30.7	11.9	9.1	1.1 (21.0)	−8.0	15.2	3.3
1i	−609.3948681	29.0	11.1	9.7	0.8 (18.2)	−6.3	14.1	−0.1
1k	−609.3907333	25.9	4.8	10.4	1.2 (16.0)	−10.0	15.6	1.8

[a] Electronic energy + ZPE relative to **1**, in kcal/mol. [b] Sum-corrected difference in energy between the singlet and triplet states of diradical **A**, in kcal/mol. [c] Electronic energy + ZPE relative to **A**, in kcal/mol. Values in parentheses are relative to **B**. [d] Electronic energy + ZPE relative to **B**, in kcal/mol.

Table 3. Diplole Moments of Substituted 1,2-Dialkynylimidazoles and Bergman Cyclization Transition States

	1[a]	TS1[a]
1a	4.30	4.56
1b	2.98	3.55
1c	2.72	2.97
1e	5.94	4.55
1i	3.47	3.72
1k	2.48	2.62

[a] Dipole moments (Debye) calculated at the B3LYP/6-31G(d,p) level.

transition state. However, for the *p*-nitrophenyl analogue **1e**, for which the 1,2-dialkynylimidazole has a larger dipole moment than the Bergman transition state, the opposite solvent effect is expected. This, together with the slight increase in the Bergman cyclization barrier for **1e** relative to that of **1a**−**c** predicted from the DFT calculations (Table 2), leads to the prediction that the Bergman cyclization of **1e** in water is significantly slower than that of **1a**−**c**.

The cyclization of the 1,2-dialkynylimdiazoles **1** to the diradical intermediates **A** is predicted to be endothermic. In the case of the 4-phenyl-substituted system **1k**, the diradical is 4.8 kcal/mol higher in energy than the 1,2-dialkynylimidaozle. The cyclization is even more endothermic for the other 1,2-dialkynylimidazoles, for which the diradical **A** is 11.1−12.2 kcal/mol higher in energy than the reactant **1**.

The reactivity of benzenoid diradicals such as **A** has been proposed to correlate with the singlet−triplet (S-T) gap; the larger the energy gap between the singlet and triplet states the less reactive the diradical.[38] The S-T gaps for **A** are very similar

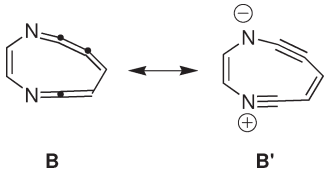

Figure 3. Resonance Structure of the intermediate **B**.

for 2-phenylethyn analogues **1a**−**c**,**e** (9.1−9.3 kcal/mol) but are slightly higher for the 1-phenylethynyl analogue **1i** (9.7 kcal/mol) and the 4-phenyl analogue **1k** (10.4 kcal/mol). In all cases, the S-T gaps for **A** are much larger than those of *p*-benzyne and related, reactive benzenoid diradicals (ca. 2−5 kcal/mol). More importantly, the barriers for the collapse of **A** to the cyclic cumulenes **B** (**TS2**) are extremely small, ranging from just 0.8 to 1.3 kcal/mol relative to **A** for **1a**,**c**,**i**, and **k** (Table 2). This leads to predictions of an exceedingly short lifetime of the diradicals **A**, which, combined with the large S-T gap for these diradicals, makes these species both fleeting and unreactive.

Interestingly, the collapse of the diradical **A** to afford the cyclic cumulene **B** is exothermic, despite the apparent strain of such a cyclic cumulene. Although strained, cyclic cumulene **B** is unexpectedly energetically stable. Using the group equivalent reaction approach[39] at the B3LYP/6-31G(d,p) level, the calculated ring strain energy (RSE) of the cyclic cumulene **B** derived from the parent 1,2-diethynylimidazole (Figure 3) is 10.7 kcal/mol, which is lower than the RSE calculated for cyclononane (16.9 kcal/mol). This relative lack of RSE can be explained by examining the resonance structure **B′** (Figure 3), which contributes significantly to the overall description of this species as evidenced by it is planar geometry, large calculated dipole (3.87 D), and short C−N bond length (1.1839 Å) for the "nitrilium" moiety. Resonance structure **B′** also emphasizes that this species has 10 π electrons and should be aromatic. Negative nucleus independent chemical shift (NICS) values are indicative of aromaticity for a wide range of hetereocycles.[40] The NICS$(1)_{zz}$ value[41] for **B** (−37.12) confirm that **B** is aromatic. Despite the contribution of the resonance from **B′**, NBO analysis[42] reveals that the B3LYP/6-31G(d,p) electron density is best represented by the Lewis structure **B** (see Supporting Information). Regioisomeric phenyl substitution of **B** has a slight effect on the energy of this species relative to **1**, with the 4-phenyl species (**Bk**) lying 10.4 kcal/mol below **1k**. The 2-phenyl-substituted case, **Bc**, is lower in energy than **1c** by 7.2 kcal/mol, and there is a stabilizing effect of further substitution on the phenyl ring only in the case of the nitro-substituted series (**Be**).

Although cumulene **B** is lower in energy than diradical **A**, the barrier for recyclization of **B** to **A** (Table 2, column **TS2**, values in parentheses) is smaller than that for this initial Bergman

dx.doi.org/10.1021/jm200289j |*J. Med. Chem.* 2011, 54, 5059–5069

cyclization. This is in contrast to the case for 2,5-didehydropyridine, for which collapse to the 2-ethynylacrylonitrile (1-aza-enediyne) is irreversible.[16] However, the intermediate **B** has an alternative cyclization mode to the carbene **C** that competes with reformation of the diradical **A** (Figure 2). This cyclization of **B** to carbene **C** has precedent in the cyclization of cyclonona-1,2,4,5-tetraene to pentalene carbene[43] and the more recent work of McGlinchey on the anomalous cyclization of a sterically hindered diallene to a cyclopenylidene carbene.[44] As shown in Table 2, **TS3** which leads to carbene **C** is in all cases lower in energy relative to **B** than **TS2**, the transition state for recyclization to the diradical **A**. This kinetic preference for cyclization to carbene **C** via **TS3** versus reformation of **A** via **TS2** is as small as 0.4 kcal/mol in the case of the 4-phenyl-substituted series **Bk** but is between 4.1−6.0 kcal/mol for the 1- and 2-phenylsubstituted series **Ba**−**c**,**e**,**i**. Thus, cyclization of cumulene **B** is predicted to lead to preferential formation of carbene **C**, which may react by a variety of pathways leading to the consumption of **B**.

Since generation of either diradical (**A**) or carbene (**C**) reactive intermediates depends upon the initial formation of the diradical **A**, the effect of substitutents on the Bergman cyclization barrier **TS1** and the nature of the diradical **A** for these substituted 1,2-dialkynylimidazoles has been examined. The relative barrier for the initial cyclization, **TS1**, is lowest for the 4-phenyl substituted analogue **1k** and highest for the *p*-nitrophenyl substituted analogue **1e**. The diradical intermediate **A** is predicted to be very short-lived in all cases, due to the low relative barrier for collapse to the cyclic cumulene **B** and the facile subsequent cyclization of **B** to the carbene **C**. However, in the case of the 4-phenyl substituted analogue **1k**, the reformation of the diradical from **B**, although kinetically disfavored, is more likely than in the case of the other analogues examined. However, the S-T splitting for the resulting diradical, **Ak**, is larger than that for the other diradicals, indicating that this species would be less reactive. Thus, it is not likely that any of these 1,2-dialkynylimidazoles react via the diradical **A**.

An alternative origin for the observed cytotoxicity of these 1,2-dialkynylimidazoles may rest in the formation of the carbenes **C**. Because the initial, rate-limiting cyclization (**TS1**) also controls the rate of formation of carbene **C**, analogue **1k**, which has the lowest relative **TS1** energy, should display enhanced cytotoxicity relative to the other analogues. Indeed, unlike the other 1,2-dialkynylimidazoles in Table 2, only **1k** is predicted to undergo cyclization at a significant rate at physiological temperature.[45] For the 1-phenylethynyl analogue **1i**, the thermodynamics of carbene formation from cumulene **B** is most favorable, and the initial cyclization (**TS1**) is lower than that of any of the 2-substituted analogues **1a**−**c**,**e**. This leads to the prediction that **1i** should be more cytotoxic than **1a**−**c**,**e**.

Kinetic Studies. In a previous communication,[25] we reported kinetic studies of the thermolysis of **1a** in 1,4-cyclohexadiene to afford products derived from trapping of carbene **Ca**. The disappearance of **1a** followed first-order kinetics, with half-lives of 135 h to 6 min at temperatures of 80 to 150 °C. The experimentally determined activation energy E_a = 30.0 kcal/mol is in excellent agreement with that predicted from the DFT calculations, 29.7 kcal/mol. We sought to expand these kinetic studies to analogues of **1a** in order to identify substituent effects on the cyclization rate and to compare these kinetic studies with the computational studies described above as well as cancer cell cytotoxcity studies (see below).

Solutions of **1a**,**b**,**e** and internal standard 5,6-benzoquinoline in 1,4-cyclohexadiene were heated at 110 °C, and the rate of disappearance of **1** was monitored by LC-MS. In all cases, the disappearance of **1** followed first-order kinetics, with half-lives ranging from 16−32 h (Table 4). There is not a strong substituent effect on the kinetics of cyclization for these three analogues; the nitro-substituted analogue **1e** has the longest half-life, which is twice as long as that for the other two analogues. Interestingly, even this modest effect of the *p*-nitrophenyl substituent is correctly predicted by the DFT calculations (Table 4), which provide an estimated E_a for the Bergman cyclization of **1e** (30.4 kcal/mol) that is just slightly higher than that predicted for **1a** and **1b** (29.6 kcal/mol in both cases).

Table 4. Comparison of Cytotoxicity, Cyclization Rates, and DFT-Predicted Cyclization Energy of Activation for a Series of 1,2-Dialkynylimidazoles

compound	IC_{50} (μM)[a]	$t_{1/2}$ (h)[b]	E_a (kcal/mol)[c]
1a	0.5 ± 0.2	17 ± 2	29.7[d]
1b	2.5 ± 0.9	16 ± 1	29.7
1c	6 ± 3	nd[e]	29.9
1d	0.5 ± 0.1	nd[e]	nd[e]
1e	0.12 ± 0.02	32 ± 1	30.5
1f	6 ± 4	nd[e]	nd[e]
1g	2.5 ± 0.9	nd[e]	nd[e]
1i	5.0 ± 0.3	nd[e]	28.9
1k	2.5 ± 0.9	nd[e]	25.8

[a] 549 cells, 72 h. [b] First-order half-life for the disappearance of dialkynylimidazole at 110 °C in neat 1,4-cyclohexadiene. [c] Predicted energy of activation ($E_a = \Delta H^{\ddagger} + RT$) for the Bergman-type cyclization at 37 °C from B3LYP/6-31G(d,p) DFT calculations. [d] Experimental E_a at 110 °C is 30.0 kcal/mol; see ref 25. [e] Not determined.

Cytotoxicity Studies. Compound **1a** was found to be cytotoxic against a range of human cancer cell lines and to induce apopotosis in the human nonsmall cell lung cancer cell line A549.[25] In order to explore the effect of 1,2-dialkynylimidazole structure on biological activity, the cytotoxicity of the 1,2-dialkynylimidazoles **1a**−**k** was determined using the AlamarBlue assay[46] against the A549 cell line (Table 4). For comparison, Table 4 also shows the experimental and computational kinetic parameters for the Bergman cyclization of a number of these 1,2-dialkynylimidazoles.

Within the 1,2-dialkynylimidazole series **1a**−**g**, the cytotoxicity against A549 cells ranges from moderate (IC_{50} ∼5−6 μM) for **1c**,**f** to high (IC_{50} = 0.12−0.5 μM) for **1a**,**d**,**e**. Both electron-withdrawing (e.g., **1e**) and electron-donating (e.g., **1a**) substituents on the phenyl ring within this series provide highly cytotoxic analogues; however, this is not uniformly the case (e.g., **1f**). The 4-substituted analogue **1k** is marginally more cytotoxic than the 1- and 2-substuted analogues **1i** and **1c**; however, **1k** is 10-fold less cytotoxic than **1a**.

These cytotoxicity results contrast with the DFT calculations and experimental half-lives for Bergman cyclization. The most cytotoxic analogue in this series, the nitrophenyl substituted compound **1e**, has the longest half-life and highest predicted E_a for Bergman cyclization. In contrast, the compound predicted to undergo Bergman cyclization most readily, **1k**, is only moderately cytotoxic. Despite nearly identical half-lives from Bergman cyclization, compounds **1a** and **1b** have IC_{50} values that differ by a factor of 5.

The contrast between the predicted facility with which these 1,2-dialkynylimidazoles undergo Bergman cyclization and their cytotoxicity against cancer cells led to a more expansive exploration

Table 5. Cytotoxicity of 1,2-Dialkynylimidazoles and Related 1- or 2-Alkynimidazoles

compound	IC_{50} (μM)
1h	1.0 ± 0.6
1j	1.9 ± 0.7
1l	2.0 ± 1.0
1m	2.6 ± 1.4
1n	2.6 ± 1.0
1o	2.0 ± 1.1
1p	2.9 ± 1.4
5a	9.2 ± 4.5
5b	>15
6b	1.1 ± 0.9
7	>15
8	10.1 ± 2.8

of the structural basis for thecytotoxicity of **1b** (Table 5). Within a wider structural range of 1,2-dialkynylimidazoles **1h**−**p**, there is little variation in cytotoxicity. Hydroxymethyl (**1j**), methoxymethyl (**1h**), and hydroxyethyl (**1n**) substitutents on the 2-alkynyl group are all well tolerated. Variations of the 4-phenyl substituent of **1k** (e.g., **1m**) or benzannulation (e.g., **1o**) are similarly well tolerated. In addition, within the 4-substituted and benzannulated series, there is little effect in going from a 2-ethynyl substituent (**1m**,**1o**) to the 2-*p*-methoxyphenethynyl substitutent (**1n**,**1p**). These results led to a more careful examination of the effect of the 1-alkynyl substituent.

Both 2-unsubstituted (**5a**) and 2-substituted (**5b**) 1-phenylethynylimidazoles are only weakly cytotoxic, as is the 1-methyl-2-alkynylimidazole **7**. However, the 1-ethynylimidazole **6b** displays cytotoxicity on par with that of the 1,2-dialkynylimidazoles **1h**−**p**. As these results implicate the 1-ethynyl group in the cytotoxicity of the 1,2-dialkynylimidazole **1a**, selective modification of this group in **1a** was explored. Interestingly, thiophenol selectively adds to the 1-ethynyl group of **1a** to afford predominantly the (*Z*)-thioenol ether **8** (Scheme 1). This modification of the 1-ethynyl group leads to greatly reduced cytotoxicity; the IC_{50} for **8** is 20-fold higher than that of **1a**.

DNA and Protein Cleavage Studies. In order to address the possible role of DNA or protein cleavage activity as a basis for the observed cytotoxicity of 1,2-dialkynylimidazoles, selected compounds were assayed for their ability to affect the cleavage of supercoiled plasmid DNA or BSA. Compounds **1a**,**e**,**m** at 100 μM concentration were incubated with supercoiled ΦX174 plasmid DNA (50 μM base pair) in 50 mM Tris buffer, pH 7.0, at 37 °C for 16 h. The resulting DNA products were separated by agarose gel electrophoresis and visualized by ethidium bromide staining. None of these compounds afforded products (relaxed circular or linear duplex) of DNA cleavage (see Supporting Information). Compound **1m** (500 μM) was incubated with 25 μM BSA in 50 mM Tris buffer, pH 7, at either 25 or 37 °C for 16 h. The resulting protein samples were analyzed by 10% SDS−PAGE and the protein products stained with Coomassie Blue. No higher-mobility bands corresponding to protein cleavage products were observed (see Supporting Information).

DISCUSSION AND CONCLUSIONS

DFT calculations of the thermal rearrangement of substituted 1,2-dialkynylimidazoles have been carried out. These calculations show that the initial Bergman cyclization is the rate-determining step. The resulting diradical is short-lived and is not expected to be reactive on the basis of the relatively large S-T gap. Collapse of the diradical to an aromatic cyclic cumulene/zwitterion is exothermic, but this species undergoes facile cyclization to a cyclopentapyrazine carbene. This overall energetic landscape is affected relatively little by substituents, with the exception of the relative height of the initial Bergman cyclization barrier. Terminal phenyl substituents on the alkyne groups raise the Bergman barrier by about 5 kcal/mol relative to the unsubstituted case, whereas phenyl substitution on the imidazole 4-position or benzannulation has little effect. A *para*-nitro substituent on the 2-phenylethynyl position has a modest effect of increasing the Bergman cyclization barrier, and even this rather small effect has been confirmed by experiment. It is interesting to note that in related benzannelated enediyne systems, the opposite trend is observed, in which electron-withdrawing substituents lower the Bergman cyclization barrier.[47] The origin of this difference in substituent effects between these two systems warrants further study. Overall, these results further support the applicability of the BS-UDFT approach for this system.

Interestingly, despite the ability of these 1,2-dialkynylimidazoles to undergo Bergman rearrangement to diradical/carbene intermediates under relatively mild conditions, there is no correlation between the rate of Bergman cyclization and cytotoxicity to A459 cells. Even 1,2-diethynylimidazoles such as **1k** that are predicted to undergo cyclization at physiological temperatures are not as cytotoxic as 1,2-dialkynylimidazoles such as **1a** that do not undergo any appreciable cyclization at this temperature. The *p*-nitrophenyl substituted 1,2-dialkynylimidazole **1e**, which undergoes cyclization at about one-half the rate of **1a**, is 4-fold more cytotoxic than **1a**.

There is no evidence that the cytotoxicity of these 1,2-dialkynylimidazoles is due to DNA cleavage or nonspecific protein cleavage. Unlike other cytoxic aza-enediyne analogues that cleave supercoiled DNA at micromolar concentrations via a hydrogen atom abstraction from the deoxyribose backbone,[22] dialkynylimidazoles **1a**,**e**,**m** do not cleave supercoiled DNA, even at 100 μM concentrations. Certain enediyne analogues have been shown to cleave a variety of proteins,[46] and hydrogen abstraction from proteins is a mechanism for self-resistance to naturally occurring enediynes.[50] However, there is no effect of 1,2-dialkynylimidazole **1m** on BSA, even at concentrations over 100-times higher than the IC_{50} for this compound.

These observations rule out a role for an unfacilitated Bergman cyclization in the cytotoxicity of these 1,2-dialkynylimidazoles. However, it is likely that 1,2-dialkynylimidazole with Bergman cyclization barriers even lower than **1k** can be designed by encompassing the dialkynes in 9- or 10-membered rings, and these may function as cytotoxic agents via spontaneous Bergman cyclization. Alternatively, 1,2-dialkynylimidazoles could be designed to undergo cyclization more rapidly when bound to DNA or proteins, leading to the production of diradical or carbene intermediates capable of modifying these binding partners. It is possible that this sort of facilitated cyclization gives rise to the enhanced cytotoxicity of certain 1,2-dialkynylimdiazoles examined here such as **1a**,**d**, and **e**. Finally, just as certain acyclic enediynes have been shown to display potent anticancer effects independent of their Bergman cyclization potential,[14] the enhanced cytotoxicity of the 1,2-dialkynylimidazoles examined here may not involve aza-Bergman cyclization at all.

An alternative or additional mechanism for the cytotoxicity of these 1,2-dialkynylimidazoles has been revealed from the study of structurally related alkynylimidazoles presented here. Although

not as cytotoxic as the 1,2-dialkynylimidazoles **1a**,**d**, and **e**, the *N*-ethynylimidazole **6b** is at least as cytotoxic as the other 1,2-dialkynylimidazoles examined. Interestingly, the *N*-ethynyl group of the 1,2-dialkynylimidazole **1a** was found to react selectively with thiophenol, and this addition abrogates the cytotoxicity of this compound. This unexpected electrophilic nature of the imidazole *N*-ethynyl group bears further study, as it stands in contrast with the established role of related *N*-alkynyl heterocycles and *N*-alkynylamides as electron-rich, nucleophilic species.[51] In light of this reactivity and the lack of DNA cleavage ability, the 1,2-dialkynylimidazoles and 1-alkynylimidazoles may have more in common with other heterocyclic, thiol-reactive anticancer agents[52] than the enediyne natural products or recently reported DNA-cleaving cytotoxic lysine−acetylene conjugates.[53] Interestingly, certain 1,2-dialkynylimidazoles such as **1a** and **1e** are notably more cytotoxic against A549 cells than thiol-reactive heterocycles currently in clinical trials.[54] Thus, the potential of *N*-ethynylimidazoles to react with biological thiols deserves further investigation, and studies exploring this possibility are ongoing.

EXPERIMENTAL SECTION

General. All reactions were carried out under argon in oven-dried glassware with magnetic stirring. Unless otherwise noted, all materials were obtained from commercial suppliers and were used without further purification. THF was distilled from sodium/benzophenone prior to use. Flash chromatography was performed with EM Reagent silica gel (230−400 mesh) using the mobile phase indicated. Melting points (open capillary) are uncorrected. Unless otherwise noted, ^{1}H and ^{13}C NMR spectra were determined in $CDCl_3$ on a spectrometer operating at 400 and 100 MHz, respectively, and are reported in ppm using solvent as the internal standard (7.26 ppm for ^{1}H and 77.0 ppm for ^{13}C in $CDCl_3$). Mass spectra were obtained in the positive mode either by chemical ionization using methane as the ionizing gas or by electrospray ionization. The purity of all test compounds was determined to by >95% by HPLC.

Typical Procedure for the Synthesis of 1,2-Dialkynylimidazoles: 1-Ethynyl-2-(2-(4-methoxyphenyl)-ethynyl)-1*H*-benzimidazole (1p). To a solution of 2-iodo-1-(2-triisopropylsilylethynyl)-1*H*-benzimidazole **4g** (212 mg, 0.5 mmol) in Et_3N (10 mL) under argon was added 4-ethynylanisole (0.075 mL, 0.55 mmol), $Pd(PPh_3)_4$ (30 mg, 0.026 mmol), and CuI (10 mg, 0.05 mmol). The reaction mixture was stirred at 50 °C until complete consumption of **4g**. The solvent was removed under reduce pressure, and the residue was purified by flash chromatography (0−5% EtOAc/hexane) to afford 210 mg (98%) of the TIPS-protected compound as a yellow crystalline solid. To this material in THF (10 mL) at −78 °C was added TBAF (0.5 mL of 1 M solution in THF, 0.5 mmol), and the mixture was stirred at −78 °C until completion. The reaction mixture was quenched at −78 °C with 10 mL of water and extracted with CH_2Cl_2 (3 × 25 mL). The organic layers were combined and dried over Na_2SO_4, and the solvent was evaporated under reduced pressure. The residue was purified by flash chromatography (0−20% EtOAc/hexane) to afford 122 mg (92%) of compound **1p** as a white solid. mp 140.1−141.3 °C; ^{1}H NMR (400 MHz, $CDCl_3$) δ 7 75 (d, J = 7.4 Hz, 1H), 7.58 (d, J = 7.4 Hz, 1H), 7.50 (d, J = 8.8 Hz, 2H), 7.37 (p, J = 7.6 Hz, 2H), 6.89 (d, J = 8.8 Hz, 2H), 3.81 (s, 3H), 3.46 (s, 1H). ^{13}C NMR (100 MHz, $CDCl_3$) δ 160.9, 141.7, 138.8, 134.6, 134.0, 125.2, 124.6, 120.4, 114.2, 112.5, 110.7, 96.6, 79.9, 69.7, 64.4, 55.3. MS (CI) 273 (M+1, 100%). HRMS calc for $C_{18}H_{13}N_2O$ ($M+H^+$) 273.1028, found 273.1028. Anal. Calcd. for $C_{18}H_{12}N_2O$: C, 79.39; H, 4.44; N, 10.20. Found: C, 79.35; H, 4.27; N, 10.18

2-(4-*tert*-Butylphenylethynyl)-1-ethynylimidazole (1b). Following the general procedure above (flash chromatography; 0−5% EtOAc/hexane), 128 mg of **1b** (75%) was obtained as a white solid. mp 82−84 °C; ^{1}H NMR (400 MHz, $CDCl_3$) δ 1.31 (s, 9H), 3.17 (s, 1H), 7.04 (d, 1H, J = 1.4 Hz), 7.14 (d, 1H, J = 1.4 Hz), 7.37 (dt, 2H, J = 8.6, 2.0 Hz), 7.51 (dt, 2H, J = 8.6, 2.0 Hz). ^{13}C NMR (100 MHz, $CDCl_3$) δ 31.1, 34.9, 61.8, 77.0, 71.1, 94.3, 118.2, 122.3, 125.5, 129.7, 131.9, 135.9, 153.1. IR (KBr) 3296, 2960, 2868, 2216, 2161, 1529, 1464, 1402, 1274, 1106, 835 cm^{-1}; MS (CI) 249 (M+1, 100%). HRMS (CI) calc for $C_{17}H_{17}N_2$ ($M + H^+$) 249.1392; found, 249.1392. Anal. Calcd. for $C_{17}H_{17}N_2$: C, 82.22; H, 6.49; N, 11.28. Found: C, 82.31; H, 6.42; N, 11.22.

2-(4-Acetylphenylethynyl)-1-ethynyl-imidazole (1d). Following the general procedure above (flash chromatography; 0−5% EtOAc/hexane), 100 mg of **1d** (73%) was obtained as a tan solid; mp 176−177 °C; ^{1}H NMR (400 MHz, $CDCl_3$) δ 2.60 (s, 3H), 3.22 (s, 1H), 7.09 (d, 1H, J = 1.6 Hz), 7.19 (d, 1H, J = 1.6 Hz), 7.66 (d, 2H, J = 8.7 Hz), 7.94 (d, 2H, J = 8.7 Hz. ^{13}C NMR (100 MHz, $CDCl_3$) δ 197.1, 137.2, 135.1, 132.1, 130.1, 128.3, 125.9, 122.8, 92.9, 80.1, 77.2, 62.2, 25; IR (KBr) 3207, 3153, 2120, 1672, 1400, 1271, 1109, 835 cm^{-1}; MS (CI) 235 (M+1, 100%). HRMS (CI) calc for $C_{15}H_{11}N_2O$ ($M + H^+$) 235.0871; found, 235.0874. Anal. Calcd. for $C_{15}H_{10}N_2O$: C, 76.91; H, 4.30; N, 11.96. Found: C, 76.40; H, 4.45; N, 11.60.

2-(4-Nitrophenylethynyl)-1-ethynylimidazole (1e). Following the general procedure above (flash chromatography; 0−5% EtOAc/hexane), 77 mg of **1e** (71%) was obtained as a yellow solid; mp 160−162 °C; ^{1}H NMR (400 MHz, $CDCl_3$) δ 3.24 (s, 1H), 7.10 (d, 1H, J = 1.2 Hz), 7.21 (d, 1H, J = 1.2 Hz), 7.37 (d, 2H, J = 9.0 Hz), 7.51 (d, 2H, J = 9.0 Hz). ^{13}C NMR (100 MHz, $CDCl_3$) δ 62.4, 70.6, 81.8, 91.6, 123.2, 123.7, 127.9, 130.4, 132.7, 134.5, 147.8. IR (KBr) 3244, 2360, 1593, 1511, 1456, 1402, 1275, 1107, 856 cm^{-1}; MS (CI) 238 (M+1, 100%). HRMS (CI) calc for $C_{13}H_8N_3O_2$ ($M + H^+$) 238.0617; found, 238.0617. Anal. Calcd. for $C_{13}H_7N_3O_2$: C, 65.82; H, 2.97; N, 17.71. Found: C, 65.65; H, 2.94; N, 17.66.

2-(3,5-Bis(trifluoromethyl)phenylethynyl)-1-ethynyl-imidazole (1g). Following the general procedure above (flash chromatography; 0−5% EtOAc/hexane), 124 mg of **1g** (68%) was obtained as a tan solid; mp 73.2−74.1 °C; ^{1}H NMR (400 MHz, $CDCl_3$) δ 3.26 (s, 1H), 7.11 (d, 1H, J = 1.6 Hz), 7.21 (d, 1H, J = 1.6 Hz), 7.87 (s, 1H), 7.98 (s, 2H). ^{13}C NMR (100 MHz, $CDCl_3$) δ 7134.3, 132.3 (q, 2C, J = 34 Hz), 131.9, 130.4 (2C), 123.2, 123.0 (q, 2C, J = 270 Hz), 122.9 (q, J = 5 Hz), 90.3, 80.3, 70.5, 62.4. IR (KBr) 2913, 2856, 2164, 1525, 1408, 1369, 1281, 1180, 1136, 899 cm^{-1}; MS (CI) 329 (M+1, 100%). HRMS (CI) calc for $C_{15}H_7N_2F_6$ ($M+H^+$) 329.0513; found, 329.0513. Anal. Calcd. for $C_{15}H_6N_2F_6$: C, 54.89; H, 1.84; N, 8.54. Found: C, 54.68; H, 1.76; N, 8.56.

3-(1-(3-Hydroxypropyn-1-yl)-1*H*-imidazol-2-yl)-prop-2-yn-1-ol (1j). The general procedure above was followed at room temperature, and the reaction mixture was quenched after 3 h with H_2O (0.2 mL). After removal of the solvent under reduced pressure, the crude was subjected to flash chromatography without extraction (flash chromatography; 0−2% MeOH/EtOAc) to afford 36 mg of **1j** (41%) as a white solid. mp 105−107 °C; ^{1}H NMR (400 MHz, MeOD-d_4) δ 7.40 (1H, d, J = 1.5 Hz), 7.02 (1H, d, J = 1.5 Hz), 4.45 (2H, s), 4.40 (2H, s). ^{13}C NMR (100 MHz, MeOD-d_4) δ 136.1, 129.9, 124.8, 95.3, 73.8, 73.4, 73.0, 50.9, 50.4. IR (KBr) 3322, 3148, 3125, 2358, 2273, 1525, 1471, 1420, 1303, 1130, 1034 cm^{-1}; MS (ESI) 375 (2M+23, 100%). HRMS (ESI) calc for $C_9H_9N_2O_2$ ($M + H^+$) 177.0654; found, 177.0658.

1,2-Diethynyl-4-phenyl-1*H*-imidazole (1k). Following the general procedure above (flash chromatography; 0−5% EtOAc/hexane), 76 mg of **1k** (79%) was obtained as a white solid. mp 62°−64 °C; ^{1}H NMR (400 MHz, $CDCl_3$) δ 7.77−7.75 (2H, m), 7.42−7.37 (3H, m), 7.33−7.28 (1H, m), 3.44 (1H, s), 3.24 (1H, s). ^{13}C NMR (100 MHz, $CDCl_3$) δ 142.1, 134.3, 131.8, 128.7 (2C), 128.1, 125.4 (2C), 117.6, 82.6, 71.6, 70.5, 62.2. IR (KBr) 3389, 3294, 3141, 2598, 2163, 2113, 1494, 1450, 1394, 1189, 1151, 748, 691 cm^{-1}; MS (CI) 193 (M+1, 100%). HRMS (CI) calc for $C_{13}H_9N_2$ ($M + H^+$) 193.0768; found, 193.0766. Anal. calcd

for $C_{13}H_8N_2 + 1/2\ H_2O$: C, 77.59; H, 4.51; N, 13.29. Found: C. 77.24; H, 4.43; N, 13.90.

1-Ethynyl-2-(2-(4-methoxyphenyl)-ethynyl)-4-phenyl-1*H*-imidazole (1l). Following the general procedure above (flash chromatography; 0−10% EtOAc/hexane), 116 mg of **1l** (78% overall yield) was obtained as a white solid. mp 84.9−85.0 °C; ^{1}H NMR (400 MHz, $CDCl_3$) δ 7.81−7.79 (2H, m), 7.56 (2H, d, J = 9.0 Hz), 7.42−7.38 (3H, m), 7.31 (1H, tt, J = 7.4, 1.4 Hz), 6.91 (2H, d, J = 9.0 Hz), 3.85 (3H, s), 3.25 (1H, s). ^{13}C NMR (100 MHz, $CDCl_3$) δ 160.6, 141.9, 135.8, 133.6 (2C), 132.0, 128.6 (2C), 127.8, 125.3 (2C), 117.1, 114.1 (2C), 113.0, 94.6, 76.2, 71.0, 62.1, 55.2. IR (KBr) 3269, 3184, 3138, 2216, 2155, 1602, 1521, 1393, 1250, 1022 cm^{-1}; MS (CI) 299 (M+1, 100%). HRMS (CI) calc for $C_{20}H_{15}N_2O$ (M + H$^+$) 299.1184; found, 299.1184. A second chromatography afforded analytically pure material. Anal. Calcd. for $C_{20}H_{14}N_2O$: C, 80.52; H, 4.73; N, 9.39. Found: C, 80.54; H, 4.55; N, 9.24.

4-(4-Fluorophenyl)-1-ethynyl-2-ethynyl-1*H*-imidazole (1m). Following the general procedure described above (flash chromatography; 0−20% EtOAc/hexane), we obtained 7.8 mg of **1m** (82% overall yield) as an off-white solid: mp 89.7−91.5 °C; ^{1}H NMR (400 MHz, $CDCl_3$) δ 7.75−7.72 (2H, m), 7.34 (1H, s), 7.10−7.06 (2H, m), 3.44 (1H, s), 3.24 (1H, s). ^{13}C NMR (100 MHz, $CDCl_3$) δ 162.6 (d, J = 246 Hz), 141.2, 134.4, 128.1 (d, J = 2.9 Hz), 127.1 (2C, d, J = 8.2 Hz), 117.2, 115.7 (2C, d, J = 21.6 Hz), 82.7, 71.5, 70.4, 62.3; MS (CI) 211 (M+1, 100%). HRMS (CI) calc for $C_{13}H_8N_2F$ (M + H$^+$) 211.0672; found, 211.0668.

4-(4-Fluorophenyl)-1(ethynyl-2-(but-3-yn-1-ol)-1*H*-imidazole (1n). Following the general procedure described above, (flash chromatography; 0−20% EtOAc/hexane) we obtained 44 mg of **1n** (35% overall yield) as a white solid: mp 146.4−148.0 °C; ^{1}H NMR (400 MHz, $CDCl_3$) δ 7.74−7.70 (2H, m), 7.30 (1H, s), 7.10−7.05 (2H, m), 3.89 (2H, t, J = 6.2 Hz), 3.23 (1H, s), 2.8 (2H, t, J = 6.2 Hz). ^{13}C NMR (100 MHz, $CDCl_3$) δ 162.6 (d, J = 246 Hz), 140.8, 135.5, 128.2 (d, J = 3 Hz), 127.0 (2C, d, J = 8.2 Hz), 116.6, 115.7 (2C, d, J = 21.6 Hz), 93.5, 70.8, 70.6, 62.0, 60.4, 23.9; MS (CI) 255 (M+1, 100%). HRMS (CI) calc for $C_{15}H_{12}N_2OF$ (M + H$^+$) 255.0934, found 255.0928.

1,2-Diethynyl-1*H*-benzimidazole (1o). Following the general procedure above (flash chromatography; 0−5% EtOAc/hexane), 66 mg of **1o** (80%) was obtained as a white solid. mp 78.1−79.2 °C; ^{1}H NMR (400 MHz, $CDCl_3$) δ 7.80−7.74 (1H, m), 7.56−7.50 (1H, m), 7.44 (1H, td, J = 7.4, 1.2 Hz), 7.38 (1H, td, J = 7.4, 1.2 Hz), 3.53 (1H, s), 3.44 (1H, s). ^{13}C NMR (100 MHz, $CDCl_3$) δ 141.2, 137.1, 134.5, 126.0, 124.9, 121.0, 111.0, 84.2, 72.0, 69.2, 64.6. IR (KBr) 3212, 2149, 2122, 1496, 1447, 1367, 1309, 1266, 1230, 1151 cm^{-1}; MS (CI) 167 (M+1, 100%). HRMS (CI) calc for $C_{11}H_7N_2$ (M + H$^+$) 167.0609; found, 167.0610. A second chromatography afforded analytically pure material. Anal. Calcd. for $C_{11}H_6N_2$: C, 79.50; H, 3.64; N, 16.86. Found: C, 79.18; H, 3.62; N, 16.64.

1-Ethynyl-4-phenyl-imidazole (6b). TBAF (1.93 mL, 1.924 mmol, of a 1 M solution in THF) was added to a solution of 623 mg of 4-phenyl-1-(triisopropylsilyl)ethynyl-1*H*-imidazole **6a**[26] in 40 mL of THF at −78 °C. The reaction mixture was stirred at −78 °C for 15 min and quenched by the addition of 3 mL of water. The reaction mixture was extracted with CH_2Cl_2 (3 × 10 mL), and the combined organic layer was dried with Na_2SO_4 and evaporated. The residue was purified by flash chromatography (50% EtOAc/hexane) to yield 291 mg (90%) of a white solid. ^{1}H NMR ($CDCl_3$): δ 7.80 (s, 1H), 7.75 (d, J = 8 Hz, 2H), 7.38 (m, 3H), 7.28 (t, J = 7.2 Hz, 1H), 3.04 (s, 1H). ^{13}C NMR (100 MHz, CDCl3): δ 141.9, 140.4, 132.5, 128.7, 127.7, 125.5, 166.6, 71,5, 59.5; MS (CI) 169 (M+1, 100%). HRMS calc for $C_{11}H_9N_2$ (M + H$^+$) 169.0766; found, 169.0766.

1-Methyl-2-((4-methoxyphenyl)ethynyl)-1*H*-imidazole (7). To a solution of 1-*tert*-butoxycarbonyl-2-iodo-1*H*-imidazole[28] (0.29 g, 1 mmol) in Et_3N (20 mL) was added 4-methoxyphenylacetylene (0.16 mL, 1.2 mmol), $Pd(PPh_3)_4$ (30 mg, 0.026 mmol), and CuI (10 mg, 0.05 mmol). The reaction mixture was stirred at 50 °C until the iodoimidazole was completely consumed. The reaction mixture was filtered. The filtrate was evaporated, and the residue was purified by flash chromatography (20% EtOAc/hexane) to afford 1-(*tert*-butoxycarbonyl)-2-((4-methoxyphenyl)-ethynyl)-1*H*-imidazole in quantitative yield. To this material (0.29 g, 1 mmol) in CH_2Cl_2 (10 mL) at −5 °C was added TFA (10 mL), and the reaction mixture was stirred at −5 °C for 2 h. The reaction mixture was neutralized with $NaHCO_3$ (20 mL) and extracted with ethyl acetate (20 mL) three times. The organic layers were combined and dried over Na_2SO_4, and the solvent was evaporated under reduced pressure. The residue was dissolved in THF (20 mL) at 0 °C, and LHMDS (1.1 mL of 1 M solution in THF, 1.1 mmol) was added. The reaction mixture was stirred at 0 °C for 30 min. To the reaction mixture was added MeI (125 μL, 2 mmol), and the reaction mixture was stirred at 0 °C until completion. The reaction mixture was quenched with water (20 mL) and extracted with CH_2Cl_2 (20 mL) three times. The organic layers were combined and dried over Na_2SO_4, and the solvent was evaporated under reduced pressure. The residue was purified by flash chromatography (50% EtOAc/hexane) to afford 1-methyl-2-((4-methoxyphenyl)ethynyl)-1*H*-imidazole **7** (123 mg, 58% yield) as white needles; mp 62−64 °C; ^{1}H NMR (400 MHz, $CDCl_3$) δ 7.49 (2H, d, J = 8.8 Hz), 7.06 (1H, d, J = 1.2 Hz), 6.91 (1H, d, J = 1.2 Hz), 6.88 (2H, d, J = 8.8 Hz), 3.82 (3H, s), 3.76 (3H, s). ^{13}C NMR (100 MHz, $CDCl_3$) δ 160.1, 133.2 (2C), 132.8, 130.6, 121.1, 114.1 (2C), 113.9, 92.6, 55.3, 33.5. IR (KBr) 3111, 1602, 1521, 1467, 1433, 1404, 1290, 1249, 1176, 1156, 1137, 1109, 1026, 843, 811, 751, 702 cm^{-1}; MS (CI) 213 (M+1, 100%). HRMS (CI) calc for $C_{13}H_{13}N_2O$ (M + H$^+$) 213.1027; found, 213.1022. Anal. Calcd. for $C_{13}H_{13}N_2O$: C, 73.56; H, 5.70; N, 13.20. Found: C, 73.47; H, 5.67; N, 13.19.

(*Z*)-2-(4-Methoxyphenyl)ethynyl-1-(2-(phenylthiol)vinyl)-1*H*-imidazole (8). To a solution of **1a** (20 mg, 0.09 mmol) in THF (2 mL) was added thiophenol (0.1 mmol, 0.01 mL). The reaction mixture was stirred at room temperature for 5 days. The reaction mixture was concentrated, and the residue was purified by flash chromatography (30% EtOAc/hexane) to afford **8** as a brown thick oil (13 mg, 43% yield). ^{1}H NMR (400 MHz, $CDCl_3$) δ 7.71 (1H, s), 7.53−7.50 (2H, m), 7.47−7.44 (2H, m), 7.39−7.35 (2H, m), 7.33−7.29 (1H, m), 7.20 (1H, d, J = 8.4 Hz), 6.91−6.88 (2H, m), 6.17 (2H, d, J = 8.4 Hz), 3.83 (3H, s). ^{13}C NMR (100 MHz, $CDCl_3$) δ 160.4, 134.3, 133.4 (2C), 132.6, 130.1 (2C), 129.4 (2C), 127.7, 121.1, 119.1, 115.5, 114.1 (2C), 113.5, 99.2, 77.2, 55.3; MS (CI) 333 (M+1, 100%). HRMS (CI) calc for $C_{20}H_{17}N_2OS$ (M + H$^+$) 333.1062; found, 333.1063.

Kinetic Study of the Thermolysis of 1,2-Dialkynylimidazoles 1a−c,e. A solution of **1** (0.05 mmol) and 5,6-benzoquinoline (0.05 mmol) in 3 mL of 1,4-cyclohexadiene was prepared. Individual aliquots (300 μL) of this solution were sealed in tubes and heated at 110 °C. At regular time periods, aliquots were removed, allowed to cool to room temperature, and subject to evaporation under vacuum. The residue was dissolved in 1 mL of an acetonitrile/water (50/50) mixture. This solution was injected in a Thermo-Finnigan LTQ XL LC-MS using a C_{18} short pad column. The analytes were eluted at 0.5 mL/min using a gradient (5−95%) of acetonitrile in water over 4 min followed by 95% acetonitrile for 1.5 min with MS detection. The mass spectra were recorded in positive mode using ESI as the ionization technique and subsequently analyzed using the software Xcalibur. Plots of peak-area-ratio of the starting 1,2-dialkynylimidazoles **1** versus time were subjected to nonlinear least-squares fitting to obtain first-order rate constants.

Supercoiled Plasmid DNA Cleavage Assay. The DNA cleavage efficiency for these 1,2-dialkynylimidazoles was determined by incubation with solutions of supercoiled (Form I) ΦX174 plasmid DNA (Fermentas, 50 μM base pairs) in 50 mM *N,N,N*-tris(hydroxymethyl)-aminomethane (Tris) buffer at pH 7. The reaction mixtures containing 100 μM test compound, 100 μM 1-propargyl-2-(2-(4-methoxyphenyl)ethynyl)pyridinium triflate[22a] as positive control, or vehicle (13% (v/v) DMSO) were incubated for 16 h at 37 °C. DNA products were separated by agarose gel electrophoresis [1× Tris-borate-*N,N,N′,N′*-ethylenediaminetetraacetic acid (EDTA) (TBE) at 90 V for 1 h] and

stained with ethidium bromide (0.25 μg/mL), and the images were analyzed using a fluorimager with ImageQuant software. The degree of cleavage of Form I DNA was determined using eq 1.

$$\text{Percent cleavage} = \frac{(2 \times [\text{Form III}] + [\text{Form II}])}{(2 \times [\text{Form III}] + [\text{Form II}] + [\text{Form I}])} \times 100 \quad (1)$$

where Form II refers to relaxed, circular DNA, and Form III is linear, duplex DNA. The reported, normalized percent cleavage accounts for cleavage in control samples under the reaction conditions employed, and this was calculated according to eq 2.

$$\text{Normalized percent cleavage} = \frac{\%\text{cleavage(drug)} - \%\text{cleavage(control)}}{100 - \%\text{cleavage control}} \quad (2)$$

Protein Cleavage Assay. Bovine serum albumin (25 μM, Fisher Bioreagent) was incubated alone or with 0.5 mM of 1,2-dialkynylimidazole **1m** in 50 mM Tris buffer at pH 7 at 25 or 37 °C for 16 h. The protein samples were analyzed by 10% SDS−PAGE and stained with Coomassie Blue.

■ ASSOCIATED CONTENT

Supporting Information. Coordinates for all stationary points, RSE calculation, Wiberg bond orders for **B**, and DNA and protein cleavage gels. This material is available free of charge via the Internet at http://pubs.acs.org.

■ AUTHOR INFORMATION

Corresponding Author
*Phone: +1-512-471-5074. Fax: +1-512-232-2606. E-mail: skerwin@mail.utexas.edu.

■ ACKNOWLEDGMENT

We are grateful to the Robert Welch Foundation (F-1298), the Texas Advanced Research Program (3658-003), and the Cancer Prevention Research Institute of Texas for financial support of this research. We thank M. Allison and E. N. Chugh for their participation in this work.

■ ABBREVIATIONS USED

BSA, bovine serum albumin; DFT, density functional theory; LHMDS, lithium bis(trimethylsilyl)amide; MAPK, mitogen-activated protein kinase; NBO, natural bond order; NICS, nucleus-independent chemical shift; RSE, ring strain energy; TBDMS, *t*-butyldimethylsilyl; TFA, trifluoroaetic acid; THF, tetrahydrofuran; TIPS, triisopropylsilyl; TMS, trimethylsilyl, Tris, *N*,*N*,*N*-tris(hydroxymethyl)aminomethane

■ REFERENCES

(1) Lee, M. D.; Manning, J. K.; Williams, D. R.; Kuck, N. A.; Testa, R. T.; Borders, D. B. Calicheamicins, a novel family of antitumor antibiotics. 3. Isolation, purification and characterization of calicheamicin-β_1^{Br}, calicheamicin-γ_1^{Br}, calicheamicin-α_2^I, calicheamicin-α_3^I, calicheamicin-β_1^I, calicheamicin-γ_1^I and calicheamicin-δ_1^I. *J. Antibiot.* **1989**, *42*, 1070–1087.

(2) Golik, J.; Dubay, G.; Groenewold, G.; Kawaguchi, H.; Konishi, M.; Krishnan, B.; Ohkuma, H.; Saitoh, K.; Doyle, T. W.; Esperamicins, A. Novel class of potent antitumor antibiotics 0.3. Structures of esperamicins-A1, esperamicin-A^2, and esperamicin- A_1^b. *J. Am. Chem. Soc.* **1987**, *109*, 3462–3464.

(3) Konishi, M.; Ohkuma, H.; Matsumoto, K.; Tsuno, T.; Kamei, H.; Miyaki, T.; Oki, T.; Kawaguchi, H.; Vanduyne, G. D.; Clardy, J.; Dynemicin, A.; Novel, A. Antibiotic with the anthraquinone and 1,5-diyn-3-ene subunit. *J. Antibiot.* **1989**, *42*, 1449–1452.

(4) Kerwin, S. M. In *Radical and Radical Ion Reactivity in Nucleic Acid Chemistry*; Greenberg, M., Ed.; Wiley: New York, 2009; pp 389−419.

(5) Rawat, D. S.; Zaleski, J. M. Geometric and electronic control of thermal Bergman cyclization. *Synlett* **2004**, 393–421.

(6) Basak, A.; Mandal, S.; Bag, S. Chelation-controlled bergman cyclization: synthesis and reactivity of enediynyl ligands. *Chem. Rev.* **2003**, *103*, 4077–4094.

(7) Polukhtine, A.; Karpov, G.; Popik, V. V. Towards photoswitchable enediyne antibiotics: single and two-photon triggering of Bergman cyclization. *Curr. Top. Med. Chem.* **2008**, *8*, 460–469.

(8) Klein, M.; Walenzyk, T.; Konig, B. Electronic effects on the Bergman cyclisation of enediynes. A review. *Collect. Czech. Chem. Commun.* **2004**, *69*, 945–965.

(9) Sherer, E. C.; Krischner, K. N.; Pickard, F. C.; Rein, C.; Feldgus, S.; Shields, G. C. Efficient and accurate characterization of the Bergman cyclization for several enediynes including an expanded substructure of esperamicin A1. *J. Phys. Chem. B* **2008**, *112*, 16917–16934.

(10) Kraka, E.; Tuttle, T.; Cremer, D. Design of a new warhead for the natural enediyne dynemicin A. An increase of biological activity. *J. Phys. Chem. B* **2008**, *112*, 2661–2670.

(11) Brzostowska, E. M.; Hoffmann, R.; Parish, C. A. Tuning the Bergman cyclization by introduction of metal fragments at various positions of the enediyne. Metalla-Bergman cyclizations. *J. Am. Chem. Soc.* **2007**, *129*, 4401–4409.

(12) Schreiner, P. R. Monocyclic enediynes: relationships between ring sizes, alkyne carbon distances, cyclization barriers, and hydrogen abstraction reactions. Singlet-triplet separations of methyl- substituted *p*-benzynes. *J. Am. Chem. Soc.* **1998**, *120*, 4184–4190.

(13) Baroudi, A.; Mauldin, J.; Alabugin, I. V. Conformationally gated fragmentations and rearrangements promoted by interception of the Bergman cyclization through intramolecular H-abstraction: a possible mechanism of auto-resistance to natural enediyne antibiotics? *J Am. Chem. Soc.* **2010**, *132*, 967–979.

(14) (a) Lo, Y.-H.; Lin, C.-C.; Lin, C.-F.; Lin, Y.-T; Duh, T.-H.; Hong, Y.-R.; Yang, S.-H.; Lin, S.-R.; Yang, S.-C.; Chang, L.-S.; Wu, M.-J. 2-(6-Aryl-3(Z)-hexen-1,5-diynyl)anilines as a new class of potent antitubulin agents. *J. Med. Chem.* **2008**, *51*, 2682–2688. (b) Lo, Y.-H.; Lin, I.-L; Lin, C.-F.; Hsu, C.-C.; Yang, S.-H.; Lin, S.-R.; Wu, M.-J. Novel acyclic enediynes inhibit cyclin A and Cdc25C expression and induce apoptosis phenomenon to show potent antitumor proliferation. *Bioorg. Med. Chem.* **2007**, *15*, 4528–4536. (c) Lin, C.-F.; Hsieh, P.-C.; Lu, W.-D.; Chiu, H.-F.; Wo, M.-J. A. Series of enediynes as novel inhibitors of topoisomerase I. *Bioorg. Med. Chem.* **2001**, *9*, 1707–1711.

(15) (a) David, W. M.; Kerwin, S. M. Synthesis and thermal rearrangement of *C*,*N*-dialkynyl imines: a potential aza-Bergman route to 2,5-didehydropyridine. *J. Am. Chem. Soc.* **1997**, *119*, 1464–1465. (b) Feng, L.; Kumar, D.; Kerwin, S. M. An extremely facile aza-Bergman rearrangement of sterically unencumbered acyclic 3-aza-3-ene-1,5-diynes. *J. Org. Chem.* **2003**, *68*, 2234–2242.

(16) Hoffner, J.; Schottelius, M. J.; Feichtinger, D.; Chen, P. Chemistry of the 2,5-didehydropyridine biradical: computational, kinetic, and trapping studies toward drug design. *J. Am. Chem. Soc.* **1998**, *120*, 376–385.

(17) Feng, L.; Zhang, A.; Kerwin, S. M. Enediynes from aza-enediynes: *C*,*N*-dialkynyl imines undergo both aza-Bergman rearrangement and conversion to enediynes and fumaronitriles. *Org. Lett.* **2006**, *8*, 1983–1986.

(18) (a) Kraka, E.; Cremer, D. Computer design of anticancer drugs. A new enediyne warhead. *J. Am. Chem. Soc.* **2000**, *122*, 8245–8264. (b) Cramer, C. J. Bergman, aza-Bergman, and protonated aza-Bergman cyclizations and intermediate 2,5-arynes: chemistry and challenge to computation. *J. Am. Chem. Soc.* **1998**, *120*, 6261–6269.

(19) Feng, L.; Kerwin, S. M. Isolation of a cyclopropane-containing product from the rearrangement of a 3-aza-3-ene-1,5-diyne under acid catalysis. *Tetrahedron Lett.* **2003**, *44*, 3463–3466.

(20) Yang, W. Y.; Breiner, B.; Kovalenko, S. V.; Ben, C.; Singh, M.; LeGrand, S. N.; Sang, Q. X. A.; Strouse, G. F.; Copland, J. A.; Alabugin, I. V. C-Lysine conjugates: pH-controlled light-activated reagents for efficient double-stranded DNA cleavage with implications for cancer therapy. *J. Am. Chem. Soc.* **2009**, *131*, 11458–11470.

(21) Feng, L.; Kumar, D.; Birney, D.; Kerwin, S. M. α,5-Didehydro-3-picoline diradicals from skipped aza-enediynes: computational and trapping studies of an aza-myers-saito cyclization. *Org. Lett.* **2004**, *6*, 2059–2062.

(22) (a) Tuesuwan, B.; Kerwin, S. M. 2-Alkynyl-*N*-propargyl pyridinium salts: pyridinium-based heterocyclic skipped-aza-enediynes that cleave DNA by deoxyribosyl hydrogen atom abstraction and guanine oxidation. *Biochemistry* **2006**, *45*, 7265–7276. (b) Tuntiwechapikul, W.; David, W. M.; Kumar, D.; Salazar, M.; Kerwin, S. M. DNA modification by 4-aza-3-ene-1,6-diynes: DNA cleavage, pH-dependent cytosine-specific interactions, and cancer cell cytotoxicity. *Biochemistry* **2002**, *41*, 5283–5290.

(23) (a) Nadipuram, A. K.; David, W. M.; Kumar, D.; Kerwin, S. M. Synthesis and thermolysis of heterocyclic 3-aza-3-ene-1,5-diynes. *Org. Lett.* **2002**, *4*, 4543–4546. (b) Kerwin, S. M.; Nadipuram, A. 5*H*-Cyclopentapyrazines from 1,2-dialkynylimidazoles. *Synlett* **2004**, 1404–1408. (c) Nadipuram, A. K.; Kerwin, S. M. Thermal cyclization of 1,2-dialkynyl-imidazoles to imidazo[1,2-*a*]pyridines. *Tetrahedron* **2006**, *62*, 3798–3808. (d) Nadipuram, A. K.; Kerwin, S. M. Intra- and intermolecular trapping of cyclopentapyrazine carbenes derived from 1,2-dialkynylimidazoles. *Tetrahedron Lett.* **2006**, *47*, 353–356.

(24) Perrin, C. L.; Rodgers, B. L.; O'Connor, J. M. Nucleophilic addition to a p-benzyne derived from an enediyne: A new mechanism for halide incorporation into biomolecules. *J. Am. Chem. Soc.* **2007**, *129*, 4795–4799.

(25) Laroche, C.; Li, J.; Golzales, C.; David, W. M.; Kerwin, S. M. Cyclization kinetics and biological evaluation of an anticancer 1,2-dialkynylimidazole. *Org. Biomol. Chem.* **2010**, *8*, 1535–1539.

(26) Laroche, C.; Li, J.; Freyer, M. S.; Kerwin, S. M. Coupling reactions of bromoalkynes with imidazoles mediated by copper salts: synthesis of novel *N*-alkynylimidazoles. *J. Org. Chem.* **2008**, *73*, 6462–6465.

(27) Laroche, C.; Li, J.; Kerwin, S. M. Lithiation and functionalization of *N*-alkynylimidazoles at the 2-position. *Tetrahedron Lett.* **2009**, *50*, 5194–5197.

(28) Keinan, E. Frictionless Molecular Rotary Motors. PTC Appl. WO 2008096360 2008 (CAN 149:267579).

(29) Kraka, E.; Cremer, D. CCSD(T) investigation of the Bergman cyclization of enediyne - relative stability of *o*-didehydrobenzene, *m*-didehydrobenzene, and *p*-didehydrobenzene. *J. Am. Chem. Soc.* **1994**, *116*, 4929–4936.

(30) Lindh, R.; Lee, T. J.; Bernhardsson, A.; Persson, B. J.; Karlstrom, G. Extended ab-initio and theoretical thermodynamics studies of the Bergman reaction and the energy splitting of the singlet *o*-benzynes, *m*-benzynes, and *p*-benzynes. *J. Am. Chem. Soc.* **1995**, *117*, 7186–7194.

(31) Cramer, C. J. Bergman, aza-Bergman, and protonated aza-Bergman cyclizations and intermediate 2,5-arynes: chemistry and challenge to computation. *J. Am. Chem. Soc.* **1998**, *120*, 6261–6269.

(32) Grafenstein, J.; Cremer, D. Can density functional theory describe multi-reference systems? investigation of carbenes and organic biradicals. *Phys. Chem. Chem. Phys.* **2000**, *2*, 2091–2103.

(33) Sherer, E. C.; Kirschner, K. N.; Pickard, F. C.; Rein, C.; Feldgus, S.; Shields, G. C. Efficient and accurate characterization of the Bergman cyclization for several enediynes including an expanded substructure of esperamicin A(1). *J. Phys. Chem. B* **2008**, *112*, 16917–16934.

(34) Becke, A. D. Density-functional thermochemistry 0.3. The role of exact exchange. *J. Chem. Phys.* **1993**, *98*, 5648–5652.

(35) Lee, C. T.; Yang, W. T.; Parr, R. G. Development of the Colle-Salvetti correlation-energy formula into a functional of the electron-density. *Phys. Rev. B* **1988**, *37*, 785–789.

(36) Grafenstein, J.; Hjerpe, A. M.; Kraka, E.; Cremer, D. An accurate description of the Bergman reaction using restricted and unrestricted dft: stability test, spin density, and on-top pair density. *J. Phys. Chem. A* **2000**, *104*, 1748–1761.

(37) Frisch, M. J.; Trucks, G. W.; Schlegel, H. B.; Scuseria, G. E.; Robb, M. A.; Cheeseman, J. R.; Scalmani, G.; Barone, V.; Mennucci, B.; Petersson, G. A.; Nakatsuji, H.; Caricato, M.; Li, X.; Hratchian, H. P.; Izmaylov, A. F.; Bloino, J.; Zheng, G.; Sonnenberg, J. L.; Hada, M.; Ehara, M.; Toyota, K.; Fukuda, R.; Hasegawa, J.; Ishida, M.; Nakajima, T.; Honda, Y.; Kitao, O.; Nakai, H.; Vreven, T.; Montgomery, J. A., Jr.; Peralta, J. E.; Ogliaro, F.; Bearpark, M.; Heyd, J. J.; Brothers, E.; Kudin, K. N.; Staroverov, V. N.; Kobayashi, R.; Normand, J.; Raghavachari, K.; Rendell, A.; Burant, J. C.; Iyengar, S. S.; Tomasi, J.; Cossi, M.; Rega, N.; Millam, N. J.; Klene, M.; Knox, J. E.; Cross, J. B.; Bakken, V.; Adamo, C.; Jaramillo, J.; Gomperts, R.; Stratmann, R. E.; Yazyev, O.; Austin, A. J.; Cammi, R.; Pomelli, C.; Ochterski, J. W.; Martin, R. L.; Morokuma, K.; Zakrzewski, V. G.; Voth, G. A.; Salvador, P.; Dannenberg, J. J.; Dapprich, S.; Daniels, A. D.; Farkas, Ö.; Foresman, J. B.; Ortiz, J. V.; Cioslowski, J.; Fox, D. J. *Gaussian 03*; Gaussian, Inc.: Wallingford, CT, 2009.

(38) Logan, C. F.; Chen, P. Ab initio calculation of hydrogen abstraction reactions of phenyl radical and *p*-benzyne. *J. Am. Chem. Soc.* **1996**, *118*, 2113–2114.

(39) Bachrach, S. M. The group equivalent reaction. *J. Chem. Educ.* **1990**, *67*, 907–908.

(40) Fallah-Bagher-Shaidaei, H.; Wannere, C. S.; Corminboeuf, C. m.; Puchta, R.; Schleyer, P. v. R. Which NICS aromaticity index for planar π rings is best? *Org Lett.* **2006**, *8*, 863–866.

(41) Steiner, E.; Fowler, P. W.; Jennesskens, L. W. Counter-rotating ring currents in coronene and corannulene. *Angew. Chem., Int. Ed.* **2001**, *40*, 362–366.

(42) Foster, J. P.; Weinhold, F. Natural hybrid orbitals. *J. Am. Chem. Soc.* **1980**, *102*, 7211–7218.

(43) Eisenhuth, L.; Hopf, H. Gas-phase pyrolysis of *trans*-1,2-diethynylcyclobutane and *cis*-1,2-diethynylcyclobutane: new entry to C_8H_8 energy surface. *J. Am. Chem. Soc.* **1974**, *96*, 5667–5668.

(44) Banide, E. V.; Oulie, P.; McGlinchey, M. J. From allenes to tetracenes: Syntheses, structures, and reactivity of the intermediates. *Pure Appl. Chem.* **2009**, *81*, 1–17.

(45) The estimated half-life for cyclization of **1k** at 37 °C based on the calculated E_a and assuming the same pre-exponential factor as that observed for the thermolysis of **1a** (5.9×10^{12}) is 51 h.

(46) Ahmed, S. A.; Gogal, R. M., Jr.; Walsh, J. E. A new rapid and simple nonradioactive assay to monitor and determine the proliferation of lymphocytes: an alternative to [H^3] thymidine incorporation assay. *J. Immun. Methods* **1994**, *170*, 211–224.

(47) (a) Klein, M.; Walenzyk, T.; Konig, B. Electronic effects on the Bergman cyclisation of enediynes. A review. *Collect. Czech. Chem. Commun.* **2004**, *69*, 945–965. (b) Zeidan, T. A.; Kovalenko, S. V.; Manoharan, M.; Alabugin, I. V. Ortho effect in the bergman cyclization: comparison of experimental approaches and dissection of cycloaromatization kinetics. *J. Org. Chem.* **2006**, *71*, 962–975. (c) Alabugin, I.; Breiner, B.; Manoharan, M. Cycloaromatization Reactions: The Testing Ground for Theory and Experiment. In *Advances Physical Organic Chemistry*; Richard, J. P., Ed.; Elsevier: New York, 2007; Vol. 42, pp 1−33.

(48) Fouad, F. S.; Wright, J. M.; Plourde, G.; Purohit, A. D.; Wyatt, J. K.; El-Shafey, A.; Hynd, G.; Crasto, C. F.; Lin, Y. Q.; Jones, G. B. Synthesis and protein degradation capacity of photoactivated enediynes. *J. Org. Chem.* **2005**, *70*, 9789–9797.

(49) Singh, S.; Hager, M. H.; Zhang, C. S.; Griffith, B. R.; Lee, M. S.; Hallenga, K.; Markley, J. L.; Thorson, J. S. Structural insight into the self-sacrifice mechanism of enediyne resistance. *ACS Chem. Biol.* **2006**, *1*, 451–460.

(50) Evano, G.; Coste, A.; Jouvin, K. Ynamides: versatile tools in organic synthesis. *Angew. Chem., Int. Ed.* **2010**, *49*, 2840–2859.

(51) Wondrak, G. T. Redox-directed cancer therapeutics: molecular mechanisms and opportunities. *Antioxid. Redox Signal* **2009**, *11*, 3012–3069.

(52) (a) Wells, G.; Berry, J. M.; Bradshaw, T. D.; Burger, A. M.; Seaton, A.; Wang, B.; Westwell, A. D.; Stevens, M. F. G. 4-Substituted 4-hydroxycyclohexa-2,5-dien-1-ones with selective activities against colon and renal cancer cell lines. *J. Med. Chem.* **2003**, *46*, 532–541. (b) Welsh, S. J.; Williams, R. R.; Birmingham, A.; Newman, D. J.; Kirkpatrick, D. L.; Powis, G. The thioredoxin redox inhibitors 1-methylpropyl 2-imidazolyl disulfide and pleurotin inhibit hypoxia-induced factor 1 alpha and vascular endothelial growth factor formation. *Mol. Cancer Ther.* **2003**, *2*, 235–243.

(53) (a) Yang, W. Y.; Breiner, B.; Kovalenko, S. V.; Ben, C.; Singh, M.; LeGrand, S. N.; Sang, Q. X. A.; Strouse, G. F.; Copland, J. A.; Alabugin, I. V. C-Lysine conjugates: pH-controlled light-activated reagents for efficient double-stranded DNA cleavage with implications for cancer therapy. *J. Am. Chem. Soc.* **2009**, *131*, 11458–11470. (b) Yang, W.-Y.; Cao, Q.; Callahan, C.; Galvis, C.; Sang, Q. X.; Alabugin, I. V. Intracellular DNA Damage by Lysine-Acetylene Conjugates. *J. Nucl. Acids* **2010**, DOI: 10.4061/2010/931394.

(54) Ramanathan, R. K.; Kirkpatrick, D. L.; Belani, C. P.; Friedland, D.; Green, S. B.; Chow, H. H. S.; Cordova, C. A.; Stratton, S. P.; Sharlow, E. R.; Baker, A.; Dragovich, T. A phase I pharmacokinetic and pharmacodynamic study of PX-12, a novel inhibitor of thioredoxin-1, in patients with advanced solid tumors. *Clin. Cancer Res.* **2007**, *13*, 2109–2114.